CHEMICAL ENGINEERING TRANSACTIONS
VOL. 117, 2025
A publication of AIDIC
The Italian Association of Chemical Engineering
Online at www.cetjournal.it
Guest Editors: Fabrizio Bezzo, Flavio Manenti, Gabriele Pannocchia, Almerinda di Benedetto

ISBN 979-12-81206-17-5; **ISSN** 2283-9216
DOI: 10.3303/CET25117146

Heat and Mass Transfer Study of Top-Heat-Integrated Distillation Column (T-HIDiC) using CFD

Javier A. Mancera-Apolinar[a,*], Diego F. Mendoza[b], Ronnie Andersson[c], Carlos A. M. Riascos[d]

[a]Universidad de América. Departamento de Ingeniería Química y Ambiental; tel. +57 3003865231, Avda Circunvalar No. 20-53. Bogotá-Colombia.
[b]Universidad de Antioquia. Departamento de Ingeniería Química. tel. +57 3216451100. Calle 70 # 52-21, Medellín, Antioquia.
[c]Chalmers Technology University. Department of Chemical Engineering. tel. +46 317722941. Gothenburg-Sweden.
[d]Universidad Nacional de Colombia; sede Bogotá. Departamento de Ingeniería Química y Ambiental-Grupo de Investigación de Bioprocesos; tel. +57 3125830176. Carrera 30 # 45-03; Edificio 453. Bogotá-Colombia.
javier.mancera@profesores.uamerica.edu.co

Distillation is one of the most widely used separation techniques in chemical processes, this separation method accounts for a significant portion of global energy consumption. Process intensification strategies have led to alternative technologies such as Heat Integrated Distillation Columns (HIDiC), these units can significantly reduce energy consumption. The goal of this study is to develop a CFD model to analyze momentum, heat and mass transfer in the separation of propylene/propane system in a Top HIDiC. The initial and boundary conditions are based on data from Aspen plus process simulations. Ranz-Marshall approaches are used for the representation of the heat transfer between phases and resistance in the gas phase. The mass transfer coefficient was calculated using Higbie's model implemented via UDF. The Peng-Robinson thermodynamic equilibrium model was implemented to estimate equilibrium ratio at the interface by UDF. The developed CFD model was used to evaluate three pairs of internal rectification stage plus external stripping stage, that are thermally integrated. These stages were selected as representative of the column. Phases distribution, temperature and vapor phase Murphree efficiency were obtained as results, showing the potential of CFD models to analyze new and structurally complex units.

1. Introduction

Distillation is a widely used separation technique in the chemical industry, but it is also one of the most energy-intensive processes, significantly impacting operating costs and carbon footprint. To address this issue, energy integration has been proposed as a process intensification strategy, reducing equipment and utility requirements through heat and mass integration. In this context, the Heat-Integrated Distillation Column (HIDiC) concept has been developed, achieving diabatic operation by vapor recompression at a low compression ratio, enabling substantial energy savings. HIDiC is particularly effective for separating close-boiling mixtures, such as the propylene-propane system (Olujic et al., 2003). Previous studies demonstrated that the Top HIDiC (T-HIDiC) configuration, which thermally integrates the upper rectification stages with the stripping section, is more energy-efficient (Mancera et al., 2018). Research at institutions like the University of Delft and simulations using tools such as Aspen Plus® and Aspen Hysys® have evaluated these columns, but they often overlook critical phenomena such as fluid dynamics and heat and mass transfer effects. Computational Fluid Dynamics (CFD) approaches have been used to analyze these aspects, although prior models focused primarily on heat transfer within solid structure. This study aims to develop an advanced CFD model to analyze the operation of a T-HIDiC column for propylene/propane separation, as suggested in previous work (Mancera et al., 2018). Conventional process simulations provided temperature and concentration profiles, as well as vapor and liquid flow data, to define boundary and initial conditions for CFD analysis.

Paper Received: 27 December 2024; Revised: 4 February 2025; Accepted: 24 May 2025
Please cite this article as: Mancera-Apolinar J.A., Mendoza D.F., Andersson R., Riascos C.A.M., 2025, Heat and Mass Transfer Study of Top-Heat-Integrated Distillation Column (T-HIDiC) using CFD , Chemical Engineering Transactions, 117, 871-876 DOI:10.3303/CET25117146

2. CFD and mass transfer model

The approach of continuous liquid phase based on the small density and small spatial scales of the dispersed gas was used for the multiphase behavior. The two-equation turbulence RANS (Reynolds Averaged Navier Stokes) model for the liquid and vapor phase was used (Colombo & Fairweather, 2015). The momentum exchange is modeled to consider drag, lift, and virtual mass.

2.1 Flow equations

The implemented two-fluid approach considers both, vapor and liquid phases as continuous and their models are based on two sets of conservation equations which estimate mass, momentum, and energy. These equations are written for each phase in different works (Versteeg & Malalasekera, 1995)

2.2 Modified drag model

In this research, we use a modified drag coefficient ($C_{D,corr}$), based on the Grace model and developed by Mancera et al. (2023). This correction on drag coefficient is supported on the idea that Grace model considers the balance forces acting on a single bubble moving into the liquid, instead of a multi-bubble system where each bubble interacts with the liquid and with other bubbles. The equation used is $C_{D,corr} = F_{corr}C_D$, here, C_D is the drag coefficient calculated with Grace's model (Grace et al., 1976), and F_{corr} is the correction factor.

2.3 Heat exchange coefficient

The rate of energy transfer between phases, Q_{LG}, is a function of the temperature difference and the interfacial area, A. The equation is $Q_{LG} = \hat{h}A(T_G - T_L)$, where $\hat{h}$, represents the heat transfer coefficient between phases and is determined by Ranz-Marshall's correlation (Ranz & Marshall, 1952), based on Nusselt number, Nu:

$$Nu = \frac{\hat{h}L_G}{k_G} = 2 + 0.6Re_G^{1/2}Pr^{1/3} \tag{1}$$

here k_G is the thermal conductivity of the gas phase, L_G is a characteristic length (such as the bubble diameter), Pr and Re_G are the Prandtl number and Reynolds number of the gas phase

2.4 Species Mass Transfer

To model species mass transfer at the interphase, transport equations for each specie at each phase must be solved along with the mass, momentum, and energy equations. The transport equations for the mass fraction for light component (LK), are (similar equations are developed for the heavy component):

Vapor Phase

$$\frac{\partial(\alpha_G\rho_G Y_{LK})}{\partial t} + \nabla\cdot(\alpha_G\rho_G u_G Y_{LK}) = \nabla\cdot\left[\alpha_G\rho_G D_{LK,G}\nabla Y_{LK}\right] - S_{LG,LK} \tag{2}$$

Liquid Phase:

$$\frac{\partial(\alpha_L\rho_L X_{LK})}{\partial t} + \nabla\cdot(\alpha_L\rho_L u_L X_{LK}) = \nabla\cdot\left[\alpha_L\rho_L D_{LK,L}\nabla X_{LK}\right] + S_{LG,LK} \tag{3}$$

The interphase mass transfer term $\boldsymbol{S_{LG,LK}}$ is the interphase mass transfer rate of the light component per unit volume. It is given by $S_{LG,LK} = k_{LG}A(K\rho_L^{LK} - \rho_G^{LK})$, where A is the interfacial area per unit volume, K is the mole fraction equilibrium ratio ($y_e = K/x$), ρ_p^{LK} is the mass/volume concentration of the light component in the phase *p* (this is the nomenclature used in Fluent, and $\rho_p^{LK} = \rho_L * x_{LK}$), and where:

$$\frac{1}{k_{LG}} = \frac{1}{k_G} + \frac{K}{k_L} \tag{4}$$

Here, k_G and k_L are the volumetric individual film mass transfer coefficients of gas and liquid, respectively

2.5 Mass transfer model

Interphase species mass transfer is modeled using the two-resistance model from Ansys Fluent®. There are many theories available in the literature for the calculation of the mass transfer coefficient k_G and k_L (Lamont & Scott, 1970), however the most used are:

- Penetration theory (Higbie, 1935):

$$k_L = \frac{2}{\sqrt{\pi}}\sqrt{\frac{D_{L,LK}}{t_{e,L}}} \qquad k_G = \frac{2}{\sqrt{\pi}}\sqrt{\frac{D_{G,LK}}{t_{e,G}}} \tag{5}$$

where $t_{e,L}$ and $t_{e,G}$ are the exposure time in each phase, calculated as $t_{e,L} = \frac{d_b}{u_{rise}}$ and $t_{e,G} = \frac{d_b}{u_H}$, where d_b is the bubble diameter, u_{rise} is the bubble slip velocity and u_H is the vapor velocity through the tray holes. Therefore, the expression for the local mass transfer coefficient is:

$$k_L = 2\Upsilon\sqrt{\frac{D_{L,LK}u_{rise}}{\pi d_b}} \qquad k_G = 2\Upsilon\sqrt{\frac{D_{G,LK}u_H}{\pi d_b}} \tag{6}$$

where Υ is a constant.

- Ranz-Marshall Model (Ranz & Marshall, 1952):

The Ranz-Marshall model uses an analogous approach to that for the Ranz-Marshall heat transfer coefficient model, and it is based on the Sherwood number:

$$Sh = \frac{k_m L_G}{D_G} = 2 + 0.6Re_G^{1/2}Sc_G^{1/3} \tag{7}$$

where k_m is the mass transfer coefficient in the gas phase, D_G is the diffusivity of the gas phase, L_G is a characteristic length (such as a bubble diameter), Sc_G and Re_G are the Schmidt and Reynolds number of the gas phase.

3. Simulation details

Two types of simulation were performed in this study to quantitatively analyze the operation of the T-HIDiC unit:

- Conventional or classic process simulation (Aspen Plus®)
- CFD Simulations (Ansys Fluent®)

3.1 Simulation in Aspen Plus

Conditions used for this setup of the process simulation are based on our previous work (Mancera et al., 2018b). The T-HIDiC unit was simulated using Aspen Plus 10. The Propylene-Propane system properties including vapor-liquid equilibrium data were estimated with Peng-Robinson's model. The simulations were performed in steady state, using isentropic efficiency in the compressor, and avoiding heat flow between system and surroundings.

3.2 CFD Simulation

For the geometrical configuration of the tray, concepts of distillation column design and data available in the literature for calculating the diameter of holes and landfills were used (Lockett, 1986). The mains details of the sieve tray used are reported in Table 1.

Table1. Geometrical parameters of the T-HIDiC simulated trays

Geometry	Stripping section **Dimension**	Rectification section **Dimension**
Outside tray diameter	0.32 m	0.2 m
Inside Diameter tray	0.22 m	--
Tray spacing	0.2 m	0.2 m
Hole diameter	0.005 m	0.005 m
Weir height	10mm	10mm
% Bubbling area	82.46 %	82.46 %
% hole area	8.33 %	8.48 %
Solid material	Steel	Steel

The column section considered for the CFD simulation is shown in Figure 1a and 1b. For the calculation of the temperature profile of the liquid within the simulation domain, 7 equidistant points were established along a central line in each plate (annular and concentric) at a height of y = 4 mm (Figure 1c), where the flow direction is from 1 to 7.

4. Methodology

In this research, for CFD simulations a two steps methodology was established:

1. Classical process simulation of the T-HIDiC unit under thermodynamic equilibrium conditions. The objective of this stage is to obtain the macroscopic conditions for each tray (flows, temperature,

concentrations, equilibrium ratio), these will be used to set up the boundary and initial conditions in CFD simulations. The T-HIDiC is initially simulated using the equilibrium conditions with the classical process simulation approach on Aspen Plus®. This process simulation was implemented aiming to get the input values for the CFD model. The results of this stage were also used for the estimation of the heat transfer rate from the rectification zone to the stripping zone. The results at stages 2, 30, and 59 in the stripping section and their respective rectifying stages (stages 3, 31, and 60) are used for the setting up of the boundary and initial conditions of the CFD simulations (Table 2), described in the following section.

2. CFD simulation of the T-HIDiC unit under non-equilibrium conditions. The objective of this second step is to obtain the conditions for three characteristic trays of the HIDiC column considering non-equilibrium conditions, these results are used to estimate phase volume fraction, temperature profile, and Murphree Efficiency.

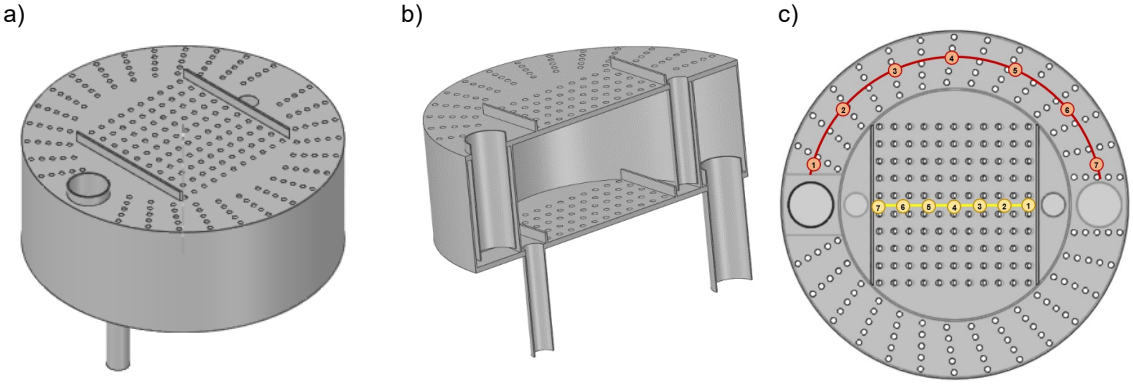

Figure 1: Geometry of the tray used for the CDF simulation of the T-HIDiC: a) Isometric view of the stage, b) Transversal section of the stage, c) Sampling points to determine temperature profile of liquid. Yellow points (rectification), red points (stripping).

5. Results

5.1 Classic process simulation

Results obtained from Aspen plus to be used in the CFD simulation are shown in Table 2 for trays 3, 31, 60 of the rectification column and trays 2, 30, and 59 of the stripping column. Equilibrium ratios are close to unity, resulting in very low relative volatility (α= [1.1 – 1.2]), which is a sign of the difficulty in separating this system.

Table 2. Values of boundary conditions for CFD simulation at selected HIDiC stages.

Area	Stage	Inlet liquid composition ($C3^=$ molar fraction)	Inlet vapor composition ($C3^=$ molar fraction)	Inlet velocity liquid (m/s)	Inlet velocity vapor (m/s)	Inlet liquid temperature (K)	Inlet vapor temperature (K)	Molar equilibrium ratio Vapor/Liquid	
								Propylene (C3=)	Propane (C3)
upper	3 R	0,9956	0.9954	0.4781	1.3961	307.8913	307.8944	1.0003	0.9168
	2 S	0,4406	0.4544	0.4602	3.6125	300.4481	300.6408	1.0887	0.9335
middle	31 R	0,9878	0.9881	1.2071	3.0453	307.9298	307.9338	1.0011	0.9166
	30 S	0,1118	0.1156	0.2716	1.960	303.4091	303.5473	1.1734	0.9796
bottom	60 R	0,9666	0.9671	1.7241	4.1949	308.0373	308.0499	1.0030	0.9164
	59 S	0,0161	0.0154	0.1403	0.8896	304.4227	304.4599	1.2022	0.9970

5.2 CFD Simulation

The formulated CFD model for the simulations under non-equilibrium conditions of the HIDiC unit was used for a detailed analysis of the heat integration in near-real conditions of three representative trays of the column.

Phase volume fraction

Vapor phase volume fraction is shown in Figure 2, the larger volume inside the trays is take up by the vapor phase.

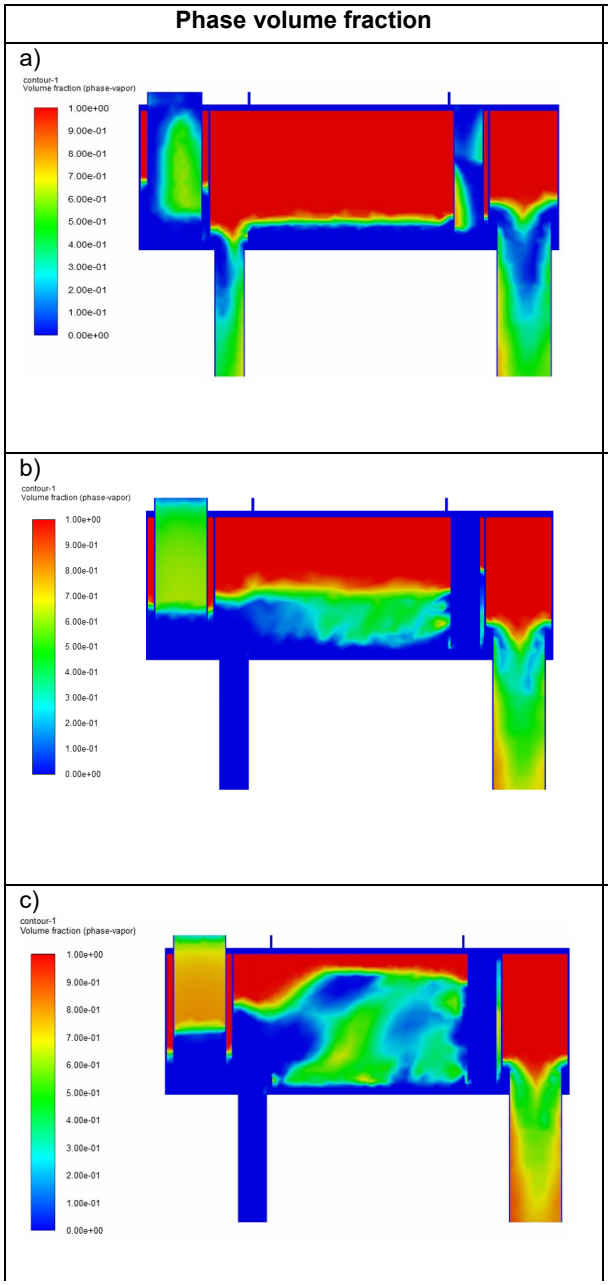

Figure 2. Phase volume fraction obtained from the CFD simulations at the three sections of HIDiC: a) upper section, b) middle section and c) bottom section.

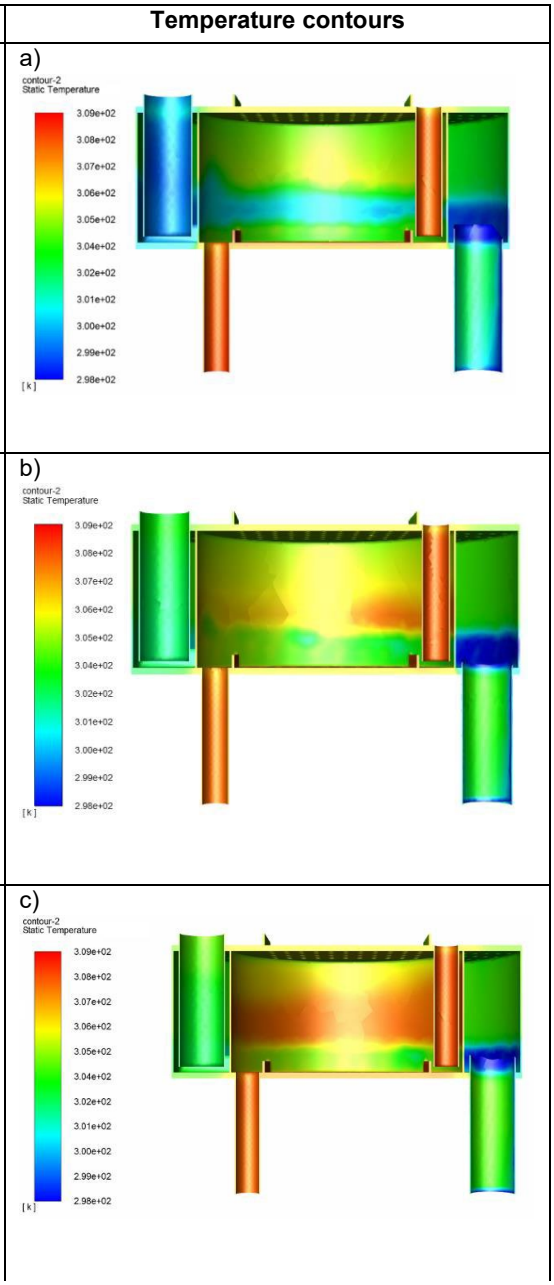

Figure 3. Temperature contours for the tray at: a) upper section, b) middle section and c) bottom section.

Temperature

Using the CFD results, temperature contours for solid structure and liquid phase in the three simulated trays under non-equilibrium conditions could be analysed. The temperature contours of the tray surface are shown in figure 3 and 4.

Murphree tray efficiency

To compare the efficiency results given by the CFD model, a simulation of the T-HIDiC in non-equilibrium was also carried out in Aspen Plus® using the Rate-Based module with the conditions defined in Table 2. Results of this simulation and its comparison with CFD results are shown in Table 3.

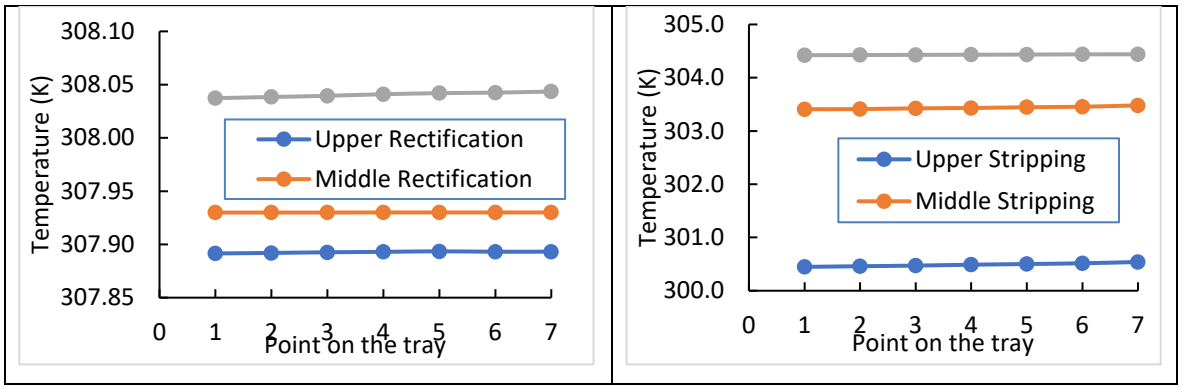

Figure 4. Temperature profiles of the liquid at 4mm on the trays (y=4mm). a) rectification trays, b) stripping trays

Table 3. Murphree efficiency results, comparison between CFD results and Rate-based model with process simulation

Tray	Section	Stage	Murphree efficiency CFD model (%)	Murphree efficiency Rate-Based model (%)
upper	Rectification	3	41.76	82.45
	Stripping	2	42.66	72.80
middle	Rectification	31	57.65	78.23
	Stripping	30	55.27	72.23
bottom	Rectification	60	37.48	76.51
	Stripping	59	40.77	69.31

6. Conclusions

The results indicated that CFD is a tool capable of predicting reliably effects of column internals geometry on the multiphase flow field and can be considered as a useful aid for the design and evaluation of the performance of the T-HIDiC column.

Acknowledgments

The authors acknowledge the financial support of Universidad Nacional de Colombia and Colciencias.

References

Colombo, M., & Fairweather, M. (2015). Multiphase turbulence in bubbly flows: RANS simulations. *International Journal of Multiphase Flow*, *77*, 222–243. https://doi.org/10.1016/j.ijmultiphaseflow.2015.09.003

Higbie, R. (1935). The rate of absorption of a pure gas into a still liquid during short periods of exposure. *Transactions of the American Institute of Chemical Engineers*, *35*, 365–389.

Grace, J. R., Wairegi, T., & Nguyen, T. H. (1976). Shapes and velocities of single drops and bubbles moving freely through immiscible liquids. In *Trans Inst Chem Eng* (Vol. 54, Issue 3)

Lockett, M. J. (1986). *Distillation tray fundamentals*. Cambridge University Press.

Mancera, J. A., Mendoza, D. F., & Riascos, C. A. M. (2018). HIDiC configuration selection based on exergetic analysis. *Chemical Engineering Transactions*, *69*, 901–906. https://doi.org/10.3303/CET1869151

Mancera-Apolinar, J. A., Mendoza, D. F., & Riascos, C. A. M. (2023). CFD Simulation and Verification of Distillation Sieve Tray Hydrodynamics by Clear Liquid Height. *Chemical Engineering Transactions*, *100*, 379–384. https://doi.org/10.3303/CET23100064

Olujic, Z., Fakhri, F., De Rijke, A., De Graauw, J., & Jansens, P. J. (2003). Internal heat integration - The key to an energy-conserving distillation column. *Journal of Chemical Technology and Biotechnology*, *78*(2–3), 241–248. https://doi.org/10.1002/jctb.761

Ranz, W. E., & Marshall, W. R. (1952). Evaporation from drops. Parts I & II. *Chem. Eng. Progr*, *48*(22).

Versteeg, H. K., & Malalasekera, W. (1995). An Introduction to Computational Fluid Dynamics The Finite Volume Method. In *Fluid flow handbook. McGraw-Hill*. Longman Scitific & Technical. https://doi.org/10.2514/1.22547